Monoclonal Antibodies to Human Erythrocyte Membrane Ca^{++}-Mg^{++} Adenosine Triphosphatase Pump Recognize an Epitope in the Basolateral Membrane of Human Kidney Distal Tubule Cells

James L. Borke,* Junzaburo Minami,‡ Anil Verma,‡ John T. Penniston,‡ and Rajiv Kumar*‡
*Department of Medicine, Divisions of Nephrology and Endocrinology, and ‡Department of Biochemistry and Molecular Biology, Mayo Clinic and Foundation, Rochester, Minnesota 55905

Abstract

Human calcium transporting tissues were examined to determine whether they contained a protein similar to the Ca^{++}-Mg^{++} adenosine triphosphatase (Ca^{++}-Mg^{++}ATPase) pump of the human erythrocyte membrane. Tissues were processed for immunoperoxidase staining using monoclonal antibodies against purified Ca^{++}-Mg^{++}ATPase. In human kidneys, specific staining was found only along the basolateral membrane of the distal convoluted tubules. Glomeruli and other segments of the nephron did not stain. Staining of erythrocytes in human spleen was readily observed. Human small intestine, human parathyroid, and human liver showed no antigens that crossreacted with the antibodies to Ca^{++}-Mg^{++}ATPase. Specific staining of distal tubule basolateral membranes from the kidney of a chimpanzee was also noted. Our experiments show, for the first time, that basolateral membranes of the human distal convoluted tubule contain a protein that is immunologically similar to the human erythrocyte Ca^{++}-Mg^{++}ATPase. These observations suggest that the cells of the distal convoluted tubules of human kidney may have a calcium pump similar to that of human erythrocyte membranes.

Introduction

Calcium-pumping ATPases of cell plasma membranes are essential elements in the control of intracellular calcium (1, 2); these calcium (Ca^{++}) pumps bind strongly to calmodulin in a number of cell types (2). The calmodulin binding properties of these enzymes have been used to construct calmodulin–Sepharose columns for the purification of such Ca^{++} ATPases. Calmodulin-sensitive Ca^{++}-Mg^{++}ATPases have been purified and studied from human erythrocytes (3), rabbit skeletal muscle (4), pig smooth muscle (5), dog heart (6), and rat brain (7). All of these enzymes form a labile phosphorylated intermediate, show an apparent molecular weight of ~ 140,000, and show an increase in the rate of Ca^{++} transport in the presence of calmodulin.

A plasma membrane Ca^{++} pump has not yet been purified from the kidney; the nature and nephron segment distribution of such a pump has not been studied systematically. No information is available on the nature of such pumps in human kidney. In basolateral membranes from pig kidney cortex, a protein of M_r = 135,000 shows the type of labile phosphorylated intermediate that is typical of plasma membrane Ca^{++} pumps. In these membranes, calmodulin also binds to a protein of the same apparent size, suggesting the presence of a calmodulin-responsive enzyme (8). A calmodulin-dependent Ca^{++}-Mg^{++}ATPase of apparent molecular weight of 142,000 has also been characterized within the kidney tubular basement membrane of rats (9). While these studies describe a Ca^{++}-ATPase in basolateral membranes of kidney tubules, they do not demonstrate the segmental distribution of this enzyme nor do they precisely identify the cellular site of such an enzyme.

Transcellular Ca^{++} transport is carried out by the cells of both the proximal and distal convoluted tubules of the kidney (10). In both cases, the direction of transport is from the luminal toward the basolateral (serosal) side of the cells. Although the proximal and distal tubules both transport Ca^{++} in the same direction, there are important differences in the character of Ca^{++} transport in these nephron segments.

First, there is co-transport of Ca^{++} and Na$^+$ in the proximal tubule, while Na$^+$ and Ca^{++} transport can be uncoupled in the distal tubule (11). The exact mechanisms whereby sodium and calcium transport are coupled in the proximal tubule are not clear. A paracellular route for proximal calcium transepithelial reabsorption and/or a basolateral Ca^{++}-Na$^+$ exchange mechanism may both play a role in this process (10).

The second major difference between Ca^{++} transport in the proximal and distal tubules is the manner in which they are regulated. Ca^{++} reabsorption in the proximal tubule is inhibited by parathyroid hormone (12, 13). This hormone and cyclic AMP have been shown to stimulate distal tubule Ca^{++} absorption and decrease Ca^{++} urinary excretion in rats (14) and rabbits (15). Studies by Law and Heath (16) have shown that at physiological doses, in vivo administration of parathyroid hormone decreases urinary calcium excretion in man.

A third difference between proximal and distal tubules is that the distal tubule has been shown in dogs to be the site of altered calcium transport in states of metabolic acidosis and alkalosis (17). In renal disorders involving predominantly the distal tubule, defects in urinary calcium excretion as well as urinary acid excretion have frequently been described (18–21).

A fourth important difference between the proximal and distal tubules is in the concentration and electrical gradients that exist between the lumen and extracellular fluid for each. Micropuncture studies in dog kidney have demonstrated only a small electrical potential across proximal tubule cells, while a large negative potential is found in the distal tubules (22). In rats and hamsters, the Ca^{++} concentration in the lumen of the

proximal tubule is also much closer to that of the extracellular fluid than is the distal tubule luminal Ca^{++} concentration (23, 24). Active transport has also been directly demonstrated in the distal tubule (11).

A fifth significant difference between the two segments is in their vitamin D–dependent calcium binding protein content. Vitamin D–dependent calcium binding protein, present in both the kidney and intestinal epithelia, is inducible by 1,25-dihydroxyvitamin D_3 and is believed to be related to Ca^{++} transport across the cell (25, 26). This protein is present in the distal convoluted tubule but not in the proximal tubule (24). We have recently shown that a 28-kD vitamin D–dependent Ca^{++} binding protein resembles other calcium-sensitive proteins, such as calmodulin in its biophysical properties; calmodulin is a major regulator of Ca^{++}-Mg^{++}ATPase activity (27).

Thus, it is apparent that important differences exist between Ca^{++} transport in the proximal and distal convoluted tubules. Despite these differences only one study to date has examined plasma membrane Ca^{++}-ATPases from different portions of the nephron (28). This study, by Doucet and Katz, measured ATPase activity in the proximal and distal tubules of the rabbit kidney. The authors found that Ca^{++} ATPase activity was highest in the distal tubule.

There is no information concerning the distribution or nature of Ca^{++}-Mg^{++}ATPases in the human kidney. In the present report, we show that monoclonal antibodies to the human erythrocyte plasma membrane Ca^{++}-Mg^{++}ATPase pump crossreact with a protein or substance within the basolateral portion of the distal convoluted tubule cells of the human kidney, but not with substances in other nephron segments. The physiological relevance of this observation lies in the implication that this distal tubular Ca^{++}-ATPase might represent a calcium pump within the human kidney, where hormone-regulated calcium movement out of the cell and into the extracellular fluid is known to occur. These studies also provide strong evidence for this Ca^{++} pump being similar to the Ca^{++} pump of human erythrocyte plasma membranes.

Methods

Purification of Ca^{++}-Mg^{++}ATPase

Ca^{++}-Mg^{++}ATPase was purified from erythrocyte ghosts using calmodulin–affinity chromatography as previously described (29).

Preparation of monoclonal antibodies

Immunization. 8–10-wk-old male BALB/c mice (Jackson Laboratory, Bar Harbor, ME) were immunized with 100 μg of purified human erythrocyte Ca^{++}-Mg^{++}ATPase in complete Freund's adjuvant. 4 wk after the primary immunization, sera from the mice were tested for the presence of antibody by an enzyme-linked immunosorbent assay (ELISA) described below. Animals with high serum antibody titers received another 50 μg of antigen intraperitoneally. 3 d later the spleen was excised for fusion.

Cells and media. The mouse myeloma cell line FO (30) was used for cell fusion. It was maintained in RPMI 1640 medium (M. A. Bioproducts, Walkersville, MD) supplemented with 10% heat-inactivated fetal calf serum (HyClone, Logan, UT), 4.5 g glucose/liter, 2 mM L-glutamine (KC Biological Inc., Lenexa, KS), 10% NCTC-135 (Gibco, Grand Island, NY), 0.1 μM sodium selenite, and 50 μg/ml gentamicin. The cell cultures were replated every 3–4 d by seeding in fresh media at a concentration of 5×10^5 cells/ml.

Cell fusion. Fusion was performed according to the protocol of Kennett et al. (31) with some modifications. Approximately 10^8 spleen cells and 2×10^7 log phase myeloma cells were mixed and then pelleted at 900 g for 5 min. The cells were washed with serum-free medium (RPMI 1640 medium supplemented with 4.5 g glucose/liter), repelleted, and then gently resuspended in 0.5 ml of 50% polyethylene glycol (PEG) (PEG 1450; J. T. Baker Chemical Co., Phillipsburg, NJ). The cells were exposed to PEG for 2 min and then 0.2 ml of serum-free medium was added four times every 1 min over the next 4 min, after which 5 ml of serum-free medium was added. All the solutions were prewarmed to 37°C and maintained at that temperature during fusion. After fusion, cells were recentrifuged at 900 g for 3 min. Cells were dispensed into 96-well microculture plates containing a macrophage feeder layer, and the medium was changed every 3 d with HAT medium (RPMI 1640 medium supplemented with 10^{-4} M hypoxanthine, 4×10^{-7} M aminopterin, 1.6×10^{-5} thymidine, 10% heat-inactivated fetal calf serum, 4.5 g/ml glucose, 2 mM L-glutamine, 10% NCTC-135, 10 mM sodium selenite, and 50 μg/ml gentamicin). The feeder cells were BALB/c macrophages obtained by peritoneal lavage with 0.34 M sucrose. 5×10^3 peritoneal exudate cells were seeded per well and allowed to attach to the microculture plates overnight before fusion.

Selection of hybridomas. After 10 to 14 d in culture, the supernatant fluids from each actively growing hybridoma were screened by an ELISA. Hybridomas producing antibody were cloned by limiting dilution.

Purification of monoclonal antibodies. Ascites fluid was produced by peritoneal injection of 3–5 $\times 10^6$ hybridoma cells into BALB/c mice which had been primed 1 wk earlier with 0.5 ml of pristane (2,6,10,14-tetramethylpentadecane; Aldrich Chemical Co., Milwaukee, WI). The ascites fluid was collected 1–2 wk later, and IgG was purified by precipitation with 45% ammonium sulfate.

Determination of monoclonal antibody sub-isotype. The subisotype of the five antibodies produced was established using a mouse monoclonal subisotyping kit in an ELISA (HyClone). Each cell culture was tested for the presence of mouse IgG1, IgG2a, IgG2b, IgG3, IgM, IgA, kappa, and lambda. Clones containing more than one subisotype were not used.

Demonstration of antibody–antigen binding

ELISA was performed by a modification of a published method (32). 100 μl of antigen at 1 μg/ml in 0.5 M carbonate buffer, pH 9.8, were dispensed into 96-well microtiter plates (Flow Laboratory, Inc., McLean, VA) and incubated overnight at 4°C. After washing with 150 μl of washing buffer (0.15 M NaCl, 20 mM Tris-HCl, pH 7.4, 0.05% Tween 20, 0.01% ovalbumin), 100 μl of diluted hybridoma culture media or ascites fluids were allowed to react with the antigen for 1 h at room temperature. The plates were washed and 100 μl of goat anti-mouse IgG antibody, conjugated to alkaline phosphatase (Pel-Freeze Biologicals, Brown Deer, WI), were added. After incubation for 1 h at room temperature and subsequent washing, 100 μl of substrate (p-nitrophenyl phosphate; Sigma Chemical Co., St. Louis, MO) in substrate buffer (1 M diethanolamine, 1 mM $MgCl_2$, 0.5 mM $ZnCl_2$, adjusted pH to 9.8 with HCl) were added. After incubation for 1 h at room temperature the absorbance at 410 nm was determined with a microplate reader (Dynatech Laboratory, Inc., Alexandria, VA).

Preparation of western blot

Electrophoresis of purified Ca^{++}-Mg^{++}ATPase. Sodium dodecyl sulfate (SDS) polyacrylamide gel electrophoresis was performed on 7.5% gels as described by Laemmli (33). Pyronin Y was used as the tracking dye as this was found to bind to nitrocellulose paper better than bromophenol blue after electrophoretic transfer.

Electrophoretic transfer. Proteins were transferred to nitrocellulose as described by Towbin et al. (34).

Binding of antibody to nitrocellulose immobilized proteins. Immediately after the transfer, the nitrocellulose paper was immersed in a Tris buffer saline solution containing 5% bovine serum albumin. The paper was then treated with appropriate antibodies by the method of Burnette (35). Binding was assessed by the detection of a colored prod-

uct produced by peroxidase-conjugated antibodies in the presence of 4-chloro-1-napthol plus H_2O_2.

Ca^{++}-$Mg^{++}ATPase$ assay

The activity of Ca^{++}-Mg^{++}ATPase was quantified by measuring the liberation of inorganic phosphate from [γ-^{32}P]ATP at 37°C (36). All assays were run for 30 min in triplicate in media containing 5.0 mM EDTA, 25 mM N-tris[hydroxymethyl]methyl-2-aminoethane sulfonic acid-triethylamine (pH 7.4 at 37°C), 1.6 mM $CaCl_2$ (5.0 μM free Ca^{++}), 9.0 mM $MgCl_2$, 6.0 mM ATP, and 1 μg of purified ATPase. Where calmodulin was added, 0.5 μg was used. Monoclonal antibodies and a normal IgG control were added at 0.1, 1.0, 10, and 100 μg of appropriate antibody per reaction.

Protein determinations

The method of Lowry et al. (37) as modified by Bensadoun and Weinstein (38) was used to determine protein concentrations in all samples. Bovine serum albumin was the standard used for these determinations.

Tissue selection

Human tissues obtained from surgery and autopsy were fixed immediately in 10% formalin overnight. Tissue blocks were selected from autopsy specimens where the time between death and autopsy was < 6 h. All animal specimens were fixed immediately after killing.

Samples from six human intestine, thirteen human kidney, three human parathyroid, seven human spleen, and four human liver tissues were processed for study. In addition, intestine, kidney, spleen, and liver from a 200-g male Sprague-Dawley rat, as well as kidney from a 5-kg male pig-tail macaque monkey, a 10-kg male dog, and a 56-kg male chimpanzee, were also processed.

Immunohistochemistry

Tissues for localization studies were processed using the avidin–biotin procedure of Hsu et al. (39). All tissue was fixed in a 10% phosphate-buffered formalin solution and dehydrated in a graded series of ethanol and xylene washes before embedding in paraffin. 5-μm sections were placed on glass slides. The tissues were heat fixed to the slides at 55°C for 2 h and deparaffinized in D-limonene (Sigma Chemical Co.) for 5 min. The tissue sections are rehydrated with two washes with 100% ethanol, followed by 95% ethanol, and two washes of phosphate-buffered saline, pH 7.4 (PBS), for 3 min each. Endogenous peroxidase activity was blocked with 3% hydrogen peroxide for 5 min. Nonspecific antibody binding was blocked by exposure of the section to a 1:75 dilution of normal horse serum for 20 min (Vector Laboratories, Inc., Burlingame, CA). The sections were then incubated for 30 min in a humid chamber with a 1:500 dilution of mouse ascites fluid containing monoclonal antibodies to human erythrocyte Ca^{++}-Mg^{++}ATPase. Tissues incubated in ascites fluid without antibody to Ca^{++}-Mg^{++}ATPase were used as negative controls. After rinsing in PBS, the sections were incubated for 30 min in a 1:200 dilution of biotinylated horse anti–mouse IgG (Vector Laboratories, Inc.). The sections were again rinsed and incubated for 30 min in a solution containing 45 μl of avidin–peroxidase solution A, 45 μl of avidin–peroxidase solution B, and 5 ml of PBS (Vector Laboratories, Inc.). Sections were rinsed thoroughly in PBS and incubated for 10 min in a PBS solution containing 0.05 M 3,3'-diaminobenzidine tetrahydrochloride grade II (Sigma Chemical Co.) plus 0.03% hydrogen peroxide.

After 10 min, the slides were rinsed in water, counterstained for 5 min with Mayer's hematoxylin, dipped in ammonia water and rinsed for 10 min. Tissue sections were then dehydrated in ethanol and xylene and coverslipped with Permount. All slides were photographed on a Zeiss microscope using Kodak VPL film.

Periodic acid–Shiff's (PAS) technique

Kidney tissue sections were stained by the PAS technique of Mac-Manus (40). This technique specifically stains basement membranes and carbohydrates and allows the differentiation of proximal tubules from other segments of the nephron based on luminal brush border membrane staining.

Results

Subisotyping of the mouse monoclonal antibodies showed them all to be of the IgG1 type.

Western blots of three of the mouse monoclonal antibodies demonstrated that they were directed toward a protein with the characteristics of the Ca^{++} pumping ATPase (Fig. 1). The major band at 138 kD represents the monomer of the erythrocyte Ca^{++} pump (29). The strong staining of this band by all three antibodies clearly demonstrates that they are directed against the Ca^{++} pump. These Western blots were done using the purified Ca^{++} pump, and were somewhat overloaded, disclosing three minor bands which also crossreacted with the monoclonal antibodies. The crossreaction of these bands confirms our long-standing observation that they also represent forms of the Ca^{++} pump. In the case of the band migrating immediately above the monomer (at 170–200 kD), previous evidence has shown that it forms a Ca^{++}-dependent labile phosphorylated intermediate, as does the 138-kD Ca^{++} pump (3). It appears likely that this higher molecular weight band represents ATPase monomer plus a tightly bound peptide cleaved from another molecule of ATPase. The remainder of this second ATPase molecule is presumably the lower molecular weight component that appears below the intact ATPase molecule on the Western blot. The band at the origin of the gel probably represents ATPase aggregates that do not enter the gel.

The interaction of the antibodies with purified enzyme is further shown in the ELISA titration (Fig. 2). All of the antibodies showed strong color development, with JA8 and JA9 showing the highest affinity for the enzyme; both of them developed half the maximum color at $\sim$ 8 ng of antibody per well. JA3 and JA7 showed half-maximal color development at $\sim$ 40 ng antibody/well, while JA10 required 0.4 μg/well. Each
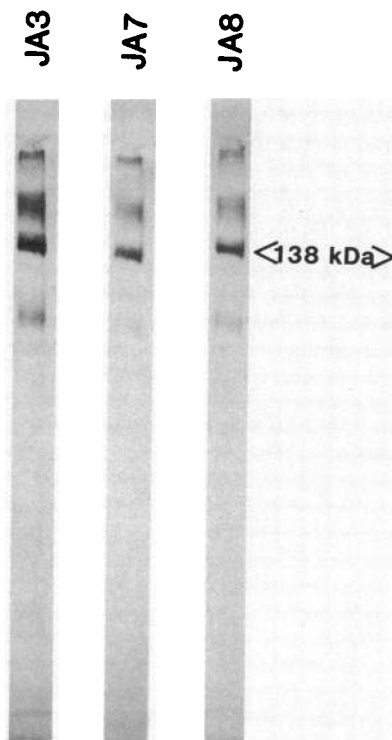

JA3 JA7 JA8

<138 kDa>

Figure 1. Western blot analysis of mouse monoclonal antibodies to Ca^{++}-Mg^{++} ATPase. 10 μg of purified Ca^{++}-Mg^{++}ATPase was electrophoresed in each lane of a 7.5% SDS–polyacrylamide gel.
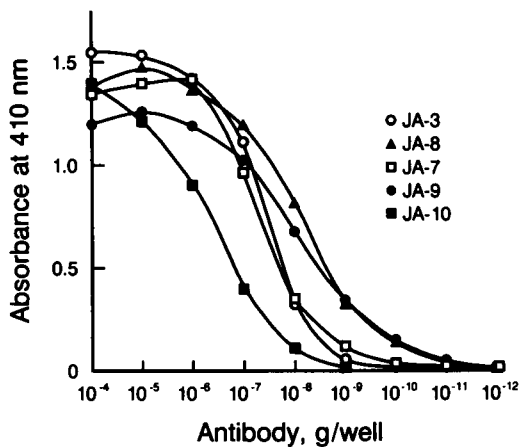
Figure 2. Chromogen absorbance at 410 nm OD versus concentration of monoclonal antibody in an ELISA system.

well contained 0.1 μg of purified human erythrocyte Ca^{++}-pumping ATPase.

The effect of three of the monoclonal antibodies on Ca^{++}-Mg^{++}ATPase activity was also tested (Table I). 1 μg of purified Ca^{++}-Mg^{++}ATPase protein was present in each assay. While calmodulin was found to produce a two- to four-fold increase in ATPase activity, amounts of antibody comparable to the amount of Ca^{++}-Mg^{++}ATPase present had only minor effects on the activity. No inhibitory effect was seen by any of the three antibodies tested. High concentrations of the antibodies JA3 and JA8 produced a two- to threefold stimulation of Ca^{++}-Mg^{++}ATPase activity when compared with controls in the presence or absence of calmodulin. Antibody JA10 had only a relatively small effect.

Five monoclonal antibodies to erythrocyte Ca^{++}-Mg^{++}ATPase were tested for tissue immunoreactivity. Table II summarizes the data on all human and animal specimens tested. Of the five antibodies tested, only the two designated JA3 and JA8 were found to crossreact with tissues. In all cases, the staining specificity and intensity were found to be identical for both antibodies. With the exception of chimpanzee distal tubule, no staining of nonhuman tissue was observed with any antibody tested. Specificity of staining was established by comparing antibody-treated sections and sections treated with antibody-negative ascites fluid. Intensity of staining was evaluated on a ± scale, where positive staining of the greatest intensity was designated ++++ and the weakest positive staining was designated +. No staining was designated −.

In the kidney, specific staining ++ to ++++ was found

Table I. Effect of Monoclonal Antibodies on the Activity of the Purified Human Erythrocyte Ca^{++} Pump

Antibody (100 μg)	Activity [nmol Pi liberated/mg · min]	
	− Calmodulin	+ Calmodulin
None	152	476
Normal IgG	144	439
JA3	310	903
JA8	355	785
JA10	134	597

Table II. Immunoperoxidase Staining of Tissue Sections with Mouse Monoclonal Antibodies to Human Erythrocyte Ca^{++}-Mg^{++}ATPase

Tissue	Sample	Monoclonal antibodies*	
		JA3, JA8	JA7, JA9, JA10
	n		
Human			
Kidney	13	++ to ++++	−
Intestine	6	−	−
Parathyroid	3	−	NP
Spleen	7	++	−
Liver	4	−	−
Rat			
Kidney	1	−	NP
Intestine	1	−	NP
Spleen	1	−	NP
Liver	1	−	NP
Monkey			
Kidney	1	−	NP
Chimpanzee			
Kidney	1	++++	NP
Dog			
Kidney	1	−	NP

NP, Not performed.
* −, No staining; +, weak staining; ++, moderate staining; +++, strong staining; ++++, very strong staining.

along the basolateral membrane of the cells of the distal convoluted tubule (see Fig. 3, a–f). No staining was found in other segments of the nephron.

Fig. 3, g and h, demonstrates kidney tissue that was double stained by the PAS technique and the immunoperoxidase technique for Ca^{++}-Mg^{++}ATPase. The PAS technique specifically stains carbohydrates and basement membranes. In the kidney, the dense brush border found on proximal tubules is high in carbohydrate and stains a red-violet color (Fig. 3, arrows). Distal tubules, loops of Henle, and collecting ducts are not lined by a dense brush border and do not show this staining. Antibodies directed against Ca^{++}-Mg^{++}ATPase do not react with tubules that are PAS positive along luminal borders. This confirms that the antibodies are not crossreacting to proximal tubule antigens.

Suppression of endogenous peroxidase proved adequate to allow detection of specific staining of erythrocytes in the human spleen (++) relative to negative controls (Fig. 3, i and j). No specific staining of human liver, human parathyroid, or human intestine was observed.

Discussion

The monoclonal antibodies used here were raised against the human erythrocyte Ca^{++}-Mg^{++}ATPase pump. Their specificity was demonstrated by their reaction with purified Ca^{++}-Mg^{++}ATPase in an ELISA system and by their staining of the appropriate 138,000-D band in a Western blot. The failure of these antibodies to inhibit Ca^{++}-Mg^{++}ATPase activity is not surprising; monoclonal antibodies against other ion transporting ATPases also show no inhibitory effect (41).
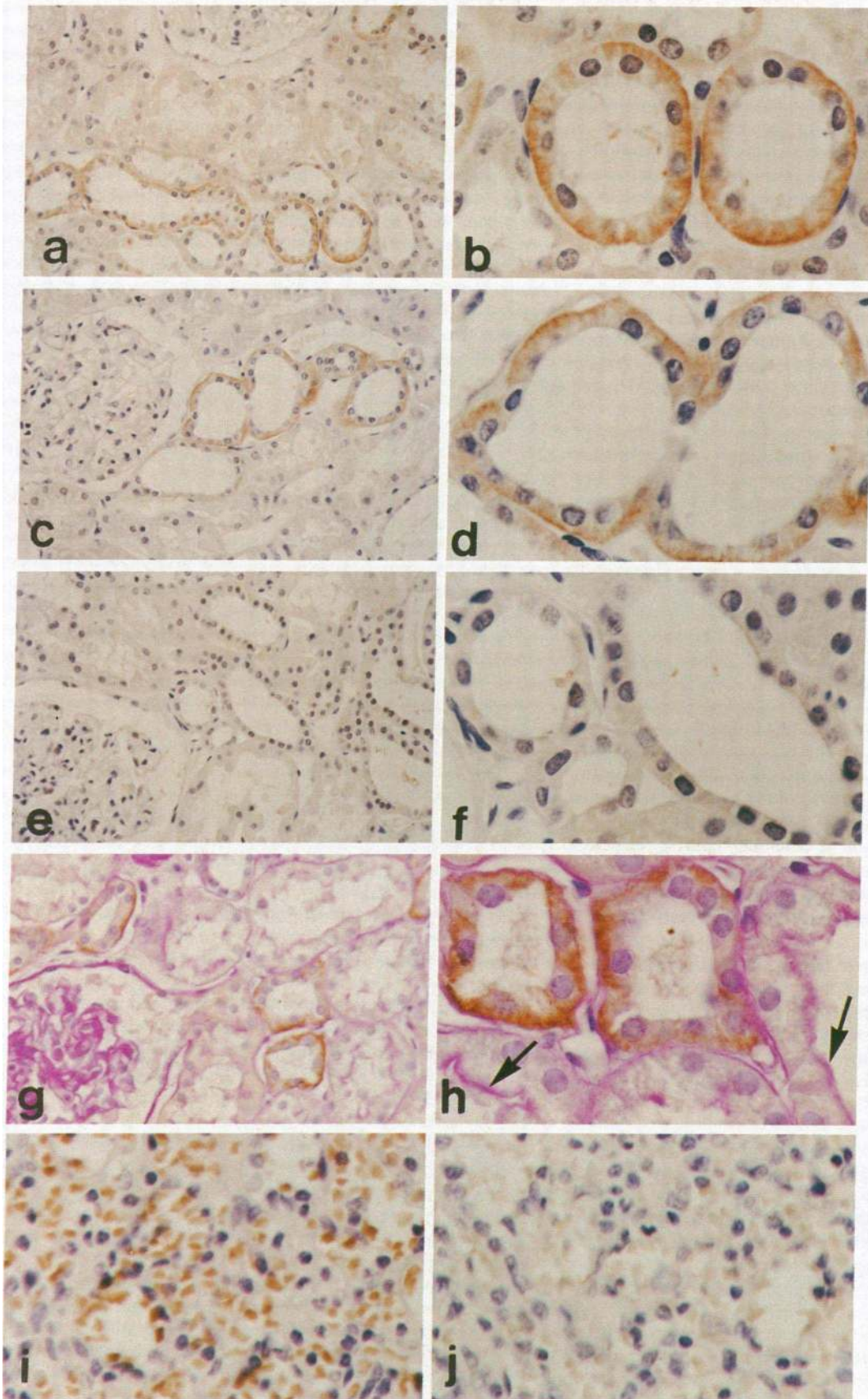
Figure 3. Immunoperoxidase localization of Ca++-Mg++ATPase within human kidney distal tubules and human spleen erythrocytes. Kidney: (*a* and *b*) Monoclonal antibody JA3. (*c* and *d*) Monoclonal antibody JA8. (*e* and *f*) Negative control. (*g* and *h*) Double stain, PAS, and JA3; (*arrows*) PAS-positive proximal tubule brush border. Spleen: (*i*) Monoclonal antibody JA3. (*j*) Negative control. (*a, c, e,* and *g*) × 200. (*b, d, f, h, i,* and *j*) × 640.

The data clearly show that antibodies JA7, JA9, and JA10 did not crossreact with any of the tissues tested. These antibodies may be directed against epitopes which do not survive the process of fixation and embedding or which are unusually labile to proteolysis. The positive results obtained with antibodies JA3 and JA8 show that human erythrocytes and human kidney distal tubule cells have an epitope in common that is lacking in other parts of the human kidney, human liver, human parathyroid, and human intestine. The absence of staining in certain tissues seems to be significant, since it is unlikely that the epitope would survive fixation and embedding in such specifically located places and not survive in all other places, including other parts of the same tissue. The absence of staining in other human tissues does not demonstrate the absence of Ca^{++} pumps similar to the erythrocyte Ca^{++}-Mg^{++}ATPase pump. The relative concentrations of the Ca^{++} pumps, however, may have some influence on their visibility by the techniques used here.

Our data demonstrate that there is a Ca^{++}-Mg^{++}ATPase–like molecule in the basolateral membranes of the cells of the distal convoluted tubule of the human kidney. As hormone-responsive calcium transport occurs in this segment of the nephron, this finding may be of importance in understanding how peptide hormones such as parathyroid hormone regulate calcium transport in this segment of the nephron. Also note that this segment of the nephron contains vitamin D–dependent calcium binding protein whereas other segments do not. The coexistence of Ca^{++}-Mg^{++}ATPase–like molecules and calcium binding protein in certain nephron segments where hormone-regulated calcium transport occurs, together with our observation that 28-kD calcium binding proteins resemble calmodulin in their biophysical properties, suggests that calcium binding proteins might regulate the activity of the Ca^{++}-Mg^{++}ATPase in this segment of the nephron in a manner analogous to calmodulin (27). Our observations suggest that the transport of calcium in different nephron segments occurs by different mechanisms. For example, it is possible that a calcium ATPase mechanism predominates in the distal nephron, whereas other mechanisms are operative in the proximal tubule.

The preferential staining of only the distal tubules and not the proximal tubules is consistent with the specialization of transport discussed in the Introduction. The implication that the kidney contains a Ca^{++}-Mg^{++}ATPase pump where hormone-regulated calcium movement is known to occur, is of physiological relevance to the understanding of the mechanism of calcium transport.

Acknowledgments

References

1. Schatzmann, H. 1975. Active calcium transport and Ca^{2+}-activated ATPase in human red cells. Curr. Top. Membr. Transp. 6:126–168.

2. Penniston, J., E. Graf, V. Niggli, A. Verma, and E. Carafoli. 1980. The plasma membrane calcium ATPase. In Calcium-binding Proteins: Structure and Function. F. Bronner and A. Kleinzeller, editors. Academic Press, Inc., New York. 23–30.

3. Niggli, V., J. Penniston, and E. Carafoli. 1979. Purification of the $(Ca^{2+}$-$Mg^{2+})$-ATPase from human erythrocyte membranes using a calmodulin affinity column. J. Biol. Chem. 254:9955–9958.

4. Michalak, M., K. Famulski, and E. Carafoli. 1984. The Ca^{2+}-pumping ATPase in skeletal muscle sarcolemma. Calmodulin dependence, regulation by cAMP-dependent phosphorylation, and purification. J. Biol. Chem. 259:15540–15547.

5. Waytack, F., G. De Schutter, and R. Casteels. 1981. Partial purification of $(Ca^{2+}$-$Mg^{2+})$-dependent ATPase from pig smooth muscle and reconstitution of an ATP-dependent Ca^{2+}-transport system. Biochem. J. 198:265–271.

6. Caroni, P., and E. Carafoli. 1981. The Ca^{2+}-pumping ATPase of heart sarcolemma. Characterization, calmodulin dependence, and partial purification. J. Biol. Chem. 256:3263–3270.

7. Hakim, G., T. Itano, A. Verma, and J. Penniston. 1982. Purification of the Ca^{2+} and Mg^{2+} requiring ATPase from rat brain synaptic plasma membrane. Biochem. J. 207:225–231.

8. Parys, J. B., H. DeSmedt, P. Vandenbergh, and R. Borghgraef. 1985. Characterization of ATP-driven calcium uptake in renal basal-lateral and renal endoplasmic reticulum membrane vesicles. Cell Calcium. 6:413–429.

9. Gmaj, P., H. Murer, and E. Carafoli. 1982. Localization and properties of a high-affinity $(Ca^{2+}$ + $Mg^{2+})$-ATPase in isolated kidney cortex plasma membranes. FEBS (Fed. Eur. Biochem. Soc.) Lett. 144:226–230.

10. Suki, W. 1979. Calcium transport in the nephron. Am. J. Physiol. 237:F1–F6.

11. Costanzo, L., and E. Windhager. 1978. Calcium and sodium transport by the distal convoluted tubule of the rat. Am. J. Physiol. 235:F492–F506.

12. Agus, Z., L. Gardner, L. Beck, and M. Goldberg. 1973. Effects of parathyroid hormone on renal tubular reabsorption of calcium, sodium and phosphate. Am. J. Physiol. 224:1143–1148.

13. Agus, Z., P. Chin, and M. Goldberg. 1977. Regulation of urinary calcium excretion in the rat. Am. J. Physiol. 232:F545–F549.

14. Costanzo, L., and E. Windhager. 1980. Effects of PTH, ADH and cyclic AMP on distal tubular Ca and Na reabsorption. Am. J. Physiol. 239:F478–F485.

15. Imai, M. 1981. Effects of parathyroid hormone and N^6, $O^{2'}$-dibutyryl cyclic AMP on Ca^{2+} transport across the rabbit distal nephron segments perfused in vitro. Pfluegers Arch. Eur. J. Physiol. 390:145–151.

16. Law, W., and H. Heath III. 1984. Time- and dose-related biphasic effects of synthetic bovine parathyroid hormone fragment 1-34 on urinary cation excretion. J. Clin. Endocrinol. Metab. 58:606–608.

17. Sutton, R., N. Wong, and J. Dirks. 1979. Effects of metabolic acidosis and alkalosis on sodium and calcium transport in the dog kidney. Kidney Int. 15:520–533.

18. Wrong, O., and H. Davies. 1959. The excretion of acid in renal disease. Q. J. Med. 28:259–314.

19. Ferris, R., M. Kashgarian, H. Levitan, I. Brandt, and F. Epstein. 1961. Renal tubular acidosis and renal potassium wasting acquired as a result of hypercalcemic nephropathy. N. Engl. J. Med. 265:924–928.

20. Morris, R., and A. Sebastian. 1983. Renal tubular acidosis and the Fanconi Syndrome. In The Metabolic Basis of Inherited Disease. 5th ed. J. Stanbury, J. Wyngaarden, D. Fredrickson, J. Goldstein, and M. Brown, editors. McGraw-Hill, Inc., New York. 1808–1843.

21. Coe, F., and J. Firpo, Jr. 1978. Evidence for mild reversible hyperparathyroidism in distal renal tubular acidosis. Arch. Intern. Med. 135:1485–1489.

22. Boulpaep, E., and J. Seely. 1971. Electrophysiology of proximal and distal tubule. Am. J. Physiol. 221:1084–1096.

23. Lassiter, W., C. Gottschalk, and M. Mylle. 1963. Micropunc-

ture study of renal tubular reabsorption of calcium in normal rodents. *Am. J. Physiol.* 204:771–775.

24. Wright, F. 1971. Increasing magnitude of electrical potential along the renal distal tubule. *Am. J. Physiol.* 220:624–638.

25. Roche, C., C. Bellaton, D. Pansu, A. Miller III, and F. Bronner. 1986. Localization of vitamin D-dependent active Ca^{2+} transport in rat duodenum and relation to CaBP. *Am. J. Physiol.* 251:G314–G320.

26. Roth, J., D. Brown, A. Norman, and L. Orci. 1982. Localization of the vitamin D-dependent calcium-binding protein in mammalian kidney. *Am. J. Physiol.* 243:F243–F252.

27. Gross, M. D., G. L. Nelsestuen, and R. Kumar. 1987. Observations on the binding of lanthanides and calcium to vitamin D-dependent chick intestinal calcium-binding protein: implications regarding calcium-binding protein function. *J. Biol. Chem.* 262:6539–6545.

28. Doucet, A., and A. Katz. 1982. High-affinity Ca-Mg-ATPase along the rabbit nephron. *Am. J. Physiol.* 242:F346–F352.

29. Graf, E., A. Verma, J. Gorski, G. Lopaschuk, V. Niggli, M. Zurini, E. Carafoli, and J. Penniston. 1982. Molecular properties of calcium-pumping ATPase from human erythrocytes. *Biochemistry.* 21:4511–4516.

30. Fazekas de St. Groth, S., and D. Scheidegger. 1980. Production of monoclonal antibodies: strategy and tactics. *J. Immunol. Methods.* 35:1–21.

31. Kennett, R., K. Denis, A. Tung, and N. Klinman. 1978. Hybrid plasmacytoma production: fusions with adult spleen cells, monoclonal spleen fragments, neonatal spleen cells and human spleen cells. *Curr. Top. Microbiol. Immunol.* 81:77–91.

32. Douillard, J., and T. Hoffman. 1983. Enzyme-linked immunosorbent assay for screening monoclonal antibody production using enzyme-labeled second antibody. *Methods Enzymol.* 92:168–174.

33. Laemmli, U. 1970. Cleavage of structural proteins during the assembly of the head of bacteriophage T_4. *Nature (Lond.).* 227:680–685.

34. Towbin, H., T. Stahelin, and J. Gordon. 1979. Electrophoretic transfer of proteins from polyacrylamide gels to nitrocellulose sheets. *Proc. Natl. Acad. Sci. USA.* 76:4350–4354.

35. Burnette, W. N. 1981. "Western blotting": electrophoretic transfer of proteins from SDS-polyacrylamide gels to unmodified nitrocellulose and radiographic detection with antibody and radioiodinated protein A. *Anal. Biochem.* 112:195–203.

36. Jarrett, H., and J. Penniston. 1977. Partial purification of the Ca^{2+}-Mg^{2+}-ATPase activator from human erythrocytes: its similarity to the activator of 3':5'-cyclic nucleotide phosphodiesterase. *Biochem. Biophys. Res. Commun.* 77:1210–1216.

37. Lowry, O., N. Rosebrough, A. Farr, and R. Randall. 1951. Protein measurement with the Folin phenol reagent. *J. Biol. Chem.* 193:265–275.

38. Beusadoun, A., and D. Weinstein. 1976. Assay of proteins in the presence of interfering materials. *Anal. Biochem.* 70:241–250.

39. Hsu, S., L. Raine, and H. Fanger. 1981. Use of avidin-biotin-peroxidase complex (ABC) in immunoperoxidase techniques: a comparison between ABC and unlabeled antibody (PAP) procedures. *J. Histochem. Cytochem.* 29:577–580.

40. McManus, J. 1948. Histological and histochemical uses of periodic acid. *Stain Technol.* 23:99–108.

41. Zubrzycka-Gaarn, E., G. MacDonald, L. Phillips, A. O. Jorgensen, and D. H. MacLennan. 1984. Monoclonal antibodies to the Ca^{2+}-Mg^{2+}-dependent ATPase of sarcoplasmic reticulum identify polymorphic forms of enzyme and indicate the presence in the enzyme of a classical high-affinity Ca^{2+} binding site. *J. Bioenerg. Biomembr.* 16:441–464.